



Published in final edited form as:

J Surg Res. 2012 November ; 178(1): 358–369. doi:10.1016/j.jss.2011.12.015.

Physiologic Responses to Severe Hemorrhagic Shock and the Genesis of Cardiovascular Collapse: Can Irreversibility Be Anticipated?

Hernando Gómez, Jaume Mesquida, Linda Hermus, Patricio Polanco, Hyung Kook Kim, Sven Zenker, Andrés Torres, Rajaie Namas, Yoram Vodovotz, Gilles Clermont, Juan Carlos Puyana, and Michael R. Pinsky

Abstract

Introduction—The causes of cardiovascular collapse (CC) during hemorrhagic shock (HS) are unknown. We hypothesized that vascular tone loss characterizes CC, and that arterial pulse pressure/stroke volume index ratio or vascular tone index (VTI), would identify CC.

Methods—14 Yorkshire-Durock pigs were bled to 30 mmHg mean arterial pressure and held there by repetitive bleeding until rendered unable to compensate (CC) or for 90 min (NoCC). They were then resuscitated in equal parts to shed volume and observed for 2 h. CC was defined as a MAP < 30 mmHg for 10 min or < 20 mmHg for 10 sec. Study variables were recorded at Baseline (B0), 30, 60, 90 min after bleeding and at resuscitation (R0), 30, and 60 min afterward.

Results—Swine were bled to 32±9% of total blood volume. Epinephrine (Epi) and VTI were low and did not change in NoCC after bleeding as compared to CC swine, in which both increased (0.97±0.22 to 2.57±1.42 mcg/dl, and 173±181 to 939±474 mmHg/ml, respectively), despite no differences in bled volume. Lactate increase rate (LIR) increased with hemorrhage and was higher at R0 for CC, but did not vary in NoCC. VTI identified CC from NoCC and Survivors from Non-survivors before CC. A large increase in LIR was coincident with VTI decrement before CC occurred.

Conclusions—Vasodilatation immediately prior to CC in severe HS occurs at the same time as an increase in LIR, suggesting loss of tone as the mechanism causing CC, and energy failure as its probable cause.

Keywords

animal model; autonomic control; lactate; vasomotor tone

Introduction

Cardiovascular collapse (CC) is thought to be the final lethal pathway of progressive traumatic hemorrhagic shock (T/HS). Its cause has not been completely elucidated, but various hypotheses based on animal and clinical research in trauma and sepsis suggests that

© 2011 Elsevier Inc. All rights reserved.

Corresponding Author: Hernando Gómez, M.D., Scaife Hall, 3550 Terrace Street, Suite 641, Pittsburgh, PA 15261, gomezh@upmc.edu.

Publisher's Disclaimer: This is a PDF file of an unedited manuscript that has been accepted for publication. As a service to our customers we are providing this early version of the manuscript. The manuscript will undergo copyediting, typesetting, and review of the resulting proof before it is published in its final citable form. Please note that during the production process errors may be discovered which could affect the content, and all legal disclaimers that apply to the journal pertain.

failure of the compensatory response mechanisms dependant on a functional autonomic balance may be the precipitating factor leading to CC.

Several potential mechanisms can explain CC in T/HS. Failure of the sympathetic drive and the underlying endocrine response may account for refractoriness to conventional resuscitation maneuvers (13, 14, 20, 21, 23, 33). Clinical studies demonstrated diminished endocrine responses to trauma, suggesting a possible role for endocrine failure (13). In addition, in sepsis, hormone replacement therapy has proven effective in reversing refractoriness to shock (1–9, 40, 43). The failure to couple the sympathetic/endocrine effectors (i.e. epinephrine) release to vascular endothelial-smooth muscle response is an alternative explanation for CC in these settings (27). Finally, cellular energy failure due to impaired mitochondrial oxidative phosphorylation could also explain the vasoplegia seen in the late stages of T/HS in a fashion similar to that reported in septic shock (29, 42).

Sympathetic and endocrine responses to shock can be quantified by measuring blood hormone levels (e.g. catecholamines, angiotensin II, and vasopressin) (36). Although these hormonal effectors exert various metabolic effects on diverse tissues, their main hemodynamic actions during shock are to differentially alter vasomotor tone, redistribute blood flow to the central compartment, and sustain effective circulating blood flow to vital organs (41). Accordingly, these sympathetic responses sustained by the adrenal glands, the kidney, and the pituitary system, if coupled to increased vasomotor tone, should reflect the effectiveness of the sympathetic response in increasing and sustaining vascular tone (37). Clinical surrogates of the magnitude of this coupled sympathetic-vasomotor tone response or its failure would be very useful for the diagnosis of cardiovascular sufficiency or insufficiency, respectively. We hypothesized that the relation between systemic arterial pulse pressure and stroke volume, as a surrogate for vasomotor tone, may help to quantify these interactions.

Due to the properties of left ventricular (LV) ejection and the elastic properties of the central arterial vascular system, the key determinants of arterial pulse pressure (PP = systolic – diastolic pressure) are stroke volume (SV) and central arterial tone. Variations in the magnitude of PP change with respect to SV will be indicative of changes in central arterial tone, which suggests that the slope of the PP/SV ratio may be a simple quantitative indicator of arterial tone. Based on this physiological principle, we defined the vascular tone index (VTI) as the ratio of arterial PP and stroke volume index (SVI) (22). We hypothesized that loss of vasomotor tone as quantified by VTI predicts CC, and that the origin of this vasoplegia is rooted in a cellular energy failure.

Methods

The study protocol was approved by the University of Pittsburgh Institutional Animal Care and Use Committee.

14 Yorkshire-Durock pigs (wt 31.6 ± 3.9 kg) were acclimatized for at least five days prior to the study. The animals were fasted overnight before the experiment but had free access to water. They were anesthetized with a 0.05 ml/kg body weight of a mixture of Ketamine, Xylazine and Telazol (at a concentration of 100mg/ml each) intramuscular injection for induction, followed by endotracheal intubation and maintenance anesthesia with isoflurane 1.0% to 2.0% during the remainder of the experiment. Swine were ventilated with a mixture of air and oxygen, with an approximate fraction of inspired oxygen (FiO_2) of 0.6 throughout the experiment. FiO_2 was increased to 1.0 during thoracotomy. A 21-ga catheter was inserted in an ear vein and 0.9N NaCl infusion at 60 ml/h plus 1ml/kg/h for every kg above

20 kg. During thoracotomy, the infusion rate was increased an additional 7 ml/kg/h to compensate for additional insensible losses.

Under aseptic conditions, a pulmonary artery catheter (Vigilance catheter, Edwards LifeSciences, Irvine, CA) was surgically inserted via the internal jugular vein and into the pulmonary artery as determined by blood pressure waveform analysis. Bolus thermodilution cardiac output was measured every 15 min and continuous cardiac output measurements were also measured and recorded. A high fidelity pressure-tipped transducer was inserted into the aortic arch via a carotid artery (Millar MPC-500, Millar Inc, Houston, TX) for continuous blood pressure monitoring. A triple lumen 18-ga catheter was surgically inserted in the femoral artery for blood sampling and blood pressure monitoring using a low volume pressure transducer (MP50, Gould Inc., Cleveland, OH). A large-bore introducer (8 Fr) was placed in the femoral vein as the blood withdrawal and infusion port for the bleeding/resuscitation protocol described below.

A left anterior thoracotomy was performed. The pericardium was opened and ultrasonic flow probes (Transonic®Flowprobe® S933, S928, Transonic systems inc. Ithaca, N.Y.) placed around the aortic and pulmonary arteries. Another high fidelity pressure tipped catheter (Millar) was inserted in the left atrium via the left atrial appendage to monitor left atrial pressure and held in place by a purse string suture. Once all the surgical procedures were completed and evidence of no surgical bleeding was confirmed heparin was infused (5000 U bolus i.v.).

Every experiment was performed by the same group of investigators, the same surgical team and in the same laboratory in order to control pre-hemorrhage events that could potentially alter our observations. Specifically, we made sure that the surgical intervention was reproducible and consistent, and that the laboratory was kept at the same temperature.

Hemorrhage, resuscitation protocol and subgroups

Figure 1 shows a schematic representation of the model. After surgery the swine were allowed to stabilize for 15 min with the measured variables taken then considered as baseline (BL). Stability was defined as a constant HR without arrhythmias, constant MAP similar to pre-thoracotomy values and no evidence of bleeding from the surgical sites. Once the stabilization period was concluded, initial baseline hemodynamic data were collected (B0). The animals were then bled through the femoral vein using a pump (Masterflex L/S-Easyload II, Model 7550-10, 10-600RPM, Barnant Co. Barrington, IL) at 60 ml/min. Shed blood was collected in a heparinized reservoir (1 unit/ml) and weighted (Sartorius AG scale, LA 4200, Göttingen, Germany). The bled blood volume was determined by the quotient of the weight of the shed blood and its density (1.1 gram/ml). The initial bleeding was continued until mean arterial pressure (MAP) decreased to 30 mmHg. Bleeding was re-initiated if MAP increased to 40 mmHg and was continued until MAP dropped to 30 mmHg.

Resuscitation was initiated when MAP decreased below 30 mmHg for 10 min or below 20 mmHg for 10 seconds. Swine reaching this definition are referred to as cardiovascular collapse (CC) animals. If the animal was capable of maintaining a MAP between 30 and 40 mmHg for more than 90 min after the initial bleed, resuscitation was also started. These pigs are referred to as no cardiovascular collapse (NoCC) animals. Hextend™ (6% Hetastarch in lactated electrolyte injection, Hospira, Inc., Lake Forest, IL) was infused as the resuscitation fluid at 60 ml/min and at room temperature.

After resuscitation of the shed volume, the swine were observed for 2 h or until subsequent decompensation and death occurred. Survival was defined as being alive at the end of the 2-h observation period.

Blood samples

The first blood sample, denoted the pre-surgical baseline sample (PreSx), was drawn from an ear vein immediately after intubation of the animals. After pulmonary artery catheterization and arterial catheterization, mixed venous blood and arterial samples were taken every 30 min after the first incision until surgery was completed (denoted as: S30, S60, etc.). The end of surgery was defined as BL. After the post-surgical stabilization period (15 min after BL and before hemorrhage was started), a baseline sample was obtained and designated as time 0 (B0). During hemorrhage, blood samples were obtained every 30 min thereafter until resuscitation started (denoted as: B30, B60 etc). The moment at which swine reached the CC definition (CC animals) or 90 min had elapsed (NoCC animals) was defined as R0 for timeline and sampling purposes. After this sample, resuscitation was initiated and samples were obtained every 30 min from then on (denoted as: R30, R60, etc). Mixed venous blood samples were immediately centrifuged at 2000 rpm (ALC Refrigerated centrifuge, PM140R) and plasma was stored at -80°C until further analysis to measure cytokines, $\text{NO}_2^-/\text{NO}_3^-$ and catecholamines. Arterial blood samples were immediately analyzed for pH, pCO_2 , pO_2 , glucose and lactate (Radiometer America Inc. Model ABL-725, Copenhagen). Delta glucose (ΔG) was calculated as the difference between glucose at BL and the glucose level at R0.

To summarize, the sampling sequence for all blood analyses was PreSx, S30-S60, etc., BL, B0-B30, etc. R0-R30, etc.

Cytokines and $\text{NO}_2^-/\text{NO}_3^-$ —Blood levels of TNF, IL-6 and IL-10 were determined using commercially available pig-specific ELISA kits (R&D Systems, Minneapolis, MN) and $\text{NO}_2^-/\text{NO}_3^-$ was measured using the nitrate reductase method (Cayman Chemical, Ann Arbor, MI).

Catecholamines—We measured epinephrine, norepinephrine and dopamine levels from mixed venous blood using high performance liquid chromatography or HPLC (Waters™ Autosampler model 717 plus, Controller model 600 and Fluid Unit model 610, Milford, MA). Samples were centrifuged at 2000 rpm, and stored at -80°C until analyzed.

Tissue O_2 saturation—Tissue O_2 saturation (StO_2) was measured on the inner thigh of all animals using near infrared spectroscopy (InSpectra probe, Hutchinson Industries, Hutchinson, MN), as previously described. (49)

Hemodynamic parameters

Hemodynamic data were recorded using customized software on the LabView™ system (National Instruments Corporation, Austin, TX).

The following formulas were used to calculate different indices:

Cardiac Index (CI) =	Cardiac output (CO)/Body surface area (BSA)
Stroke Volume Index (SVI) =	Cardiac index (CI)/Heart rate (HR)
Vascular Tone Index (VTI) =	Pulse pressure (PP)/SVI
Total Peripheral Resistance (TPR) =	MAP/CO
Arterial Oxygen Content (C_aO_2) =	Hemoglobin (Hb) x 1.34 ml O_2 /g Hb x S_aO_2
Venous Oxygen Content (C_vO_2) =	Hb x 1.34 ml O_2 /g Hb x S_vO_2

Oxygen Delivery Index (IDO ₂) =	CI x C _a O ₂ x 10 dL/L
Oxygen Consumption Index (IVO ₂) =	CI x (C _a O ₂ - C _v O ₂) x 10dL/L
Oxygen extraction rate (O ₂ ER) =	(C _a O ₂ - C _v O ₂)/C _a O ₂
Delta mean arterial pressure (Δ MAP) =	MAP(R30) - MAP(R0 [*])
BSA for the female pig =	0.0734 x Weight ^{0.656} (24)

*R0 = Time point at which resuscitation was indicated, but not yet started.

Statistical analysis

All data are reported as mean ± SD unless otherwise stated. Comparison of hemodynamic, cytokine, and catecholamine data between time points was done by the Friedman test and the Wilcoxon rank sum test for paired groups. The comparisons between survivor and non-survivor groups were performed using the Mann-Whitney test. Correlations were assessed using Pearson's correlation coefficient and results are presented as correlation coefficients (r) and p value. The reported p-values are two-sided, and significance reports a p value of < 0.05.

Results

Animal characteristics, surgical preparation and hemorrhagic model

Fourteen animals (mean wt 31.6±3.9 kg) with a calculated total blood volume (TBV) of 2134±262 ml were studied. Two of the 14 pigs, both from the CC group were excluded: one because of an error in the data electronic collection system during the experiment and the other because of profound metabolic derangement after surgery but prior to hemorrhage (lactate 6 mmol/L, HR 147 bpm and hyperthermia), presumably due to malignant hyperthermia.

The surgery lasted 182.2±27.1 min, and was not different between CC and NoCC groups (Table 1). There was a slight increment in HR in the NoCC group in the first 30 minutes of surgery, which was not statistically significant. Prior to the experiment, animals were kept in the same conditions at the animal facility. Potential explanations for this may be differences in inhaled anesthetic delivery (not monitored with end tidal gas analysis) yielding either higher levels of anesthesia with increased vasodilatation, or lighter anesthetic plain with autonomic response. Measured hemodynamic variables were stable throughout the surgical procedure. The lowest values for MAP, oxygen delivery index (DOI₂) and SvO₂ were recorded at 120 min (58±5 mmHg, 586±153 ml O₂/min/m² and 62±7%, respectively). Hemodynamic and metabolic variables did not vary significantly in both CC and NoCC animals throughout the surgical procedure (Table 1).

Swine were bled 2.1±0.8 times on average, for a mean bleeding volume of 684±167 ml (32.8±8.9% of TBV). Time to CC after stopping bleeding was 52.8±31.5 min in those animals that exhibited CC, and total duration of shock (defined as the time from the beginning of the first bleed until beginning of resuscitation) was 90.8±33.7 min (Table 1). Although the absolute bleeding volume was not different between CC and NoCC animals, the percentage of TBV bled was significantly higher in CC animals (35±8 v. 23±4%, p < 0.05). Due to protocol, time to CC or resuscitation and total duration of shock were higher in NoCC than in CC animals (Table 1).

VTI, Epinephrine and Lactate

Table 2 summarizes the hemodynamic parameters throughout the experiment for the entire cohort, as well as for both CC and NoCC groups.

Figure 2 shows how the pressure/flow relationships changed during different stages of the experiment in one CC animal. These changes were seen regardless of whether we examined MAP (Fig. 2A) or PP (Fig. 2B). Interestingly, during CC both MAP and PP decreased, while SVI remained constant (black squares). A decrement in MAP or PP without a change in flow was taken to infer a decrease in vascular tone. In support of that assumption, VTI decreased between B90 and R0 in CC animals (2.6 ± 1.4 to 1.9 ± 0.8 mm Hg/ml-beat-m², $p=0.06$) (Fig. 3). Importantly, this decrement in VTI preceded CC by 17.7 ± 20.1 min.

The vascular tone response as measured by VTI was different in CC and NoCC animals. Although there was an increase in VTI in both groups, it was significantly higher in CC animals (from 0.97 ± 0.22 to 2.57 ± 1.42 , 250% increase vs. 0.95 ± 0.02 to 1.53 ± 0.28 mm Hg/ml-beat-m², 50% increase, respectively). Furthermore, VTI was consistently higher in survivors (S) as compared to non-survivors (NS) as early as 30 min after hemorrhage (Fig. 4).

VTI increased parallel to Epi levels during the initial phase of shock. However, Epi peaked before VTI (B30, 939.7 ± 474 pg/ml, $p=0.028$ and B90, 2.13 ± 1.2 mm Hg/ml-m²-beat, $p=0.02$, respectively). More importantly, in CC animals VTI started to decrease before CC occurred (B90) without a concomitant drop in Epi (Epi levels: B60 749.3 ± 365.9 , B90 696 ± 564.8 , R0 581 ± 482.9 ; B60 – B90, $p=0.46$; B90 – R0, $p=0.14$; B60 – R0, $p=0.32$), norepinephrine or dopamine (data not shown) levels. Furthermore, $\text{NO}_2^-/\text{NO}_3^-$ did not change between BL and R0 (102.2 ± 73.5 vs. 95.7 ± 63.8 μMol respectively, difference -6.55 ± 14.3 μMol , $p=0.29$), suggesting that at least at the systemic level, circulating NO levels derived from the expression of the inducible form of NO synthase (iNOS) did not explain the observed vasodilatation seen in CC. It is worth noting that the $\text{NO}_2^-/\text{NO}_3^-$ assay is rather insensitive to assess NO derived from the expression of the endothelial form of NO synthase (eNOS), and thus we cannot conclude with regards to endothelial derived NO.

NoCC animals showed a different VTI and catecholamine pattern than CC animals. Bleeding did not cause significant increases in Epi and only one-third the increase in VTI as seen in CC animals. Specifically, VTI rose 75% at B90 (0.87 ± 0.07 to 1.53 ± 0.28 , $p=0.11$) without parallel increases in Epi (46.3 ± 80.2 to 86.7 ± 122.7 pg/ml, $p=0.32$) (Fig. 3).

As a dynamic measure of lactate production, we quantified the rate at which lactate increased (Lactate Increase Rate or LIR) between time points (i.e. B0 to B30, B30 to B60, etc.) (Fig. 5). For the entire cohort LIR increased significantly from B90 to R0, as compared to previous periods (BL to B30, 0.22 ± 0.21 ; B30 to B60, 0.15 ± 0.13 ; B60 to B90, 0.17 ± 0.12 vs. B90 to R0, 0.77 ± 0.61 mmol/L, $p=0.046$). Subgroup analysis showed that this increment was fully explained by LIR increase in CC animals (BL to B30, 0.23 ± 0.23 ; B30 to B60, 0.19 ± 0.11 ; B60 to B90, 0.18 ± 0.08 vs. B90 to R0, 2.41 ± 0.68 mmol/L, $p=0.051$), as no increment was seen in the NoCC group. Furthermore, the comparison of B90-R0 timepoint showed a higher LIR in CC versus NoCC ($p=0.034$).

As a complement of lactate and LIR analysis, we explored the trend of pH and Base Excess (BE) in both groups. BE showed a very similar pattern as pH. BE and pH were consistently higher in NoCC as compared to CC animals (Fig. 6A and B). Importantly, in NoCC animals BE did not decrease below 0 mmol/L, whereas in CC animals, it became negative as early as 30 min after beginning hemorrhage (B30).

Hemodynamic measurements and tissue O₂ delivery

The quotient of MAP and CO reflecting total peripheral resistance (TPR) increased significantly only after B60 in CC animals, whereas VTI detected changes in tone much earlier (B0-B30) while TPR did not change in NoCC animals.

DOI₂ decreased after initiation of hemorrhage in parallel with the decrease in CO because both arterial O₂ saturation and hemoglobin remained unchanged through hemorrhage and shock until B90 (data not shown). The fact that hemoglobin concentrations remained stable until B90 despite the blood loss means that vascular refill did not contribute significantly to circulating blood volume. Thus, the primary process that sustained blood pressure during hemorrhage and shock was the increased vasomotor tone with its associated blood flow redistribution (Fig. 1).

We found no differences in DOI₂, systemic oxygen consumption (VOI₂) or O₂ extraction ratio (O₂ER) between CC and NoCC (Table 2) despite profound acid-base equilibrium alterations seen only in CC animals.

Finally, StO₂, as a measure of tissue perfusion, did not track other perfusion (SvO₂, IDO₂), flow (CO, SVI) or pressure (MAP) indices during hemorrhage. Furthermore, the <75% StO₂ threshold, which was found to predict multiple organ dysfunction and mortality in shocked trauma patients (15), was never reached in our animals. StO₂ fell to approximately 60±36% in the NoCC group after resuscitation (R30). However, the analysis of the three swine showed that this drop was driven by one of the three. This animal (Pig 49) had a recorded StO₂ of 18% at R30, whereas the other two animals had 82 and 80%. Before R0, pig 49 had a StO₂ of 71%, and there were no specific signs of additional stress. However, post-resuscitation the animal developed increased work of breathing with use of accessory muscles and tachypnea, requiring increments in tidal volume and respiratory rate. Concomitantly with this, the last ABG sample drawn showed profound arterial hypoxemia with SpO₂ 61% and PaO₂ of 42 mmHg. The most likely explanation for this finding is that the animal developed a lethal cardiovascular collapse with pulmonary edema, and was ultimately in extremis as it finally expired 10 minutes after these last data points were collected.

Discussion

Our porcine model was created to explore the individual response of the animals to severe T/HS. To do so, we designed our protocol to match the effect of profound circulatory shock to a defined level of hypotension rather than to a fix volume of hemorrhage. Although it is possible that the animals that collapsed did so because of higher volumes of bleeding, the model allowed us to discern important differences in the animal's vasomotor and endocrine response. Our protocol design allowed each animal to generate an individual compensatory response accounting for inter-individual variability. The model was also severe enough so as to produce CC in the majority of animals (79%). Using this model, we compared differences in known measures of cardiovascular, metabolic, and immunological function between animals who developed CC and NoCC. Our *pre hoc* hypothesis was that differences would exist during hemorrhagic shock, CC and the response to fluid therapy between CC and NoCC groups.

Our model matched the effect of induced profound circulatory shock where the common stress was a defined level of hypotension causing decreased tissue hypoperfusion rather than a fix volume hemorrhage. This may be more clinically relevant (with obvious limitations) for several reasons. First, because uncontrolled bleeding is usually fixed to a perfusion pressure which defines the limiting pressure for continued hemorrhage. Second, because it

allows differences in cardiovascular reserve to play out differently in each animal thereby allowing us to have a hemorrhagic shock model of variable outcome but constant hypotension. Lastly, because mean arterial pressure and not volume bled, is the information available to primary and secondary responders when assessing and treating a trauma victim.

We were able to demonstrate that animals that had a more robust response to initial hemorrhage (higher MAP), and thus were bled to a higher extent (same total bled volume but higher %/kg volume bled), had a higher risk of developing CC than animals who responded with less vasoconstriction. The fact that CC animals had more episodes of controlled hemorrhage was not a consequence of technical errors or sample handling difficulties, but rather, a result of the animal's physiologic response and the hemorrhage protocol. This resembles uncontrolled bleeding in the field, as a higher MAP in response to hemorrhage will produce greater amount of hemorrhage, and thus confers translational characteristics to our model.

Our study shows that in this porcine model the hemodynamic and metabolic response to T/HS is phenotypically different in CC and NoCC animals. This was described best by the VTI, which was different between both groups at all times during hemorrhage and shock, and most importantly before the overt expression of CC. CC animals displayed a greater VTI increase than NoCC animals as early as B30, which persisted until B90. Similarly, 17.7±20.1 min before CC, CC animals showed a significant decline in VTI, whereas in NoCC animals VTI remained constant until the 90 min interval was over. This indicates that VTI may be capable of detecting underlying vasodilatation before irreversible CC occurs. These conclusions are consistent with previous studies (27, 36) and may confer VTI with predictive capacity. In this regard, VTI and LIR were the best predictors of CC development, and mortality (only VTI, Fig. 4), as compared to other parameters such as StO₂ measurement (15–17).

In addition, VTI has the advantage of being completely independent on the effect of HR on SV. Only in the setting of HR-induced changes in contractility, will VTI be affected by variation of HR and then only minimally. Regardless of how SV is created, its relationship to PP is defined by central arterial tone. The PP created by the SV is a function of central arterial compliance and resistance, such that if SV fell, pulse pressure would also fall and vice versa, maintaining VTI unchanged. Only with decreased vasomotor tone would PP decrease for the same SV. On the other hand, only with increased vasomotor tone would PP increase for the same SV, all independent of HR.

Interestingly, the decrease in VTI was not concordant with any decrease in hemoglobin or catecholamine levels or increases in NO levels. Furthermore, NoCC animals experiencing the same level of T/HS did not display relative vasodilatation despite Epi levels being lower than in CC animals. These collective data suggest that terminal vasodilatation in T/HS is due to a decreased vascular responsiveness to circulating Epi, norepinephrine or dopamine, rather than to catecholamine exhaustion (31, 36), loss of intravascular volume or NO release (28, 30, 47), and that this loss of vascular responsiveness is a determining factor of CC. An important limitation to our study is that we did not measure smooth muscle response to vasopressors and vasodilators directly, nor did we quantify vasopressin or angiotensin levels. Thus, we cannot provide direct evidence of a lack of vascular response or demonstrate vasopressin deficiency in this study. This limitation is significant since depletion of vasopressin in the first 60 min after hemorrhage is a potential mechanism of vasodilatation (31, 36).

The vascular hypo-responsiveness phenomenon has been previously described in the setting of energetic failure (29, 42) and during activation of vascular smooth muscle K_{ATP} channels

(18, 25, 27, 34, 36, 44) and subsequent membrane hyperpolarization in the context of ATP deficiency (34), acidosis (18) and hyperlactatemia (47). In support of this hypothesis also being operative in our model, we found incremental increases in LIR before vasodilatation (Fig. 5). The fact that LIR increased significantly when VTI started decreasing may be due to either a manifestation of cellular energetic failure and anaerobic metabolism or as a “wash-out” phenomenon after this initial “sub-clinical” vasodilatation occurred. Our model does not allow us to discriminate between these two mechanisms. CC animals exhibited an increase in LIR from B90 to R0 followed by vasodilatation whereas NoCC animals did not. Lactate, in the setting of hemorrhagic shock can accumulate by increased production due to anaerobic metabolism, clearance failure, or both (19). Increased lactate production may be secondary to anaerobiosis if IDO_2 is insufficient to sustain cellular respiration (10, 38). This phenomenon is often cited as a primary cause of lactic acidosis in circulatory shock states (10, 38). Our data showed no immediate significant changes in IDO_2 paralleling the rapid increase in lactate accumulation at B90-R0. However, after 30 min of bleeding (B30), IDO_2 became insufficient ($< 300 \text{ ml/min/M}^2$), and O_2ER and lactate increased ($> 50\%$ and $> 2 \text{ mmol/l}$, respectively) for at least an hour before CC occurred. These data suggest that inadequate substrate supply contributed to energetic and mitochondrial failure (42) and supports the traditional concept of O_2 debt as a determinant of cellular energetic failure (11, 35), even in the acute phase of shock. We cannot speculate further on this issue because we did not measure mitochondrial redox potentials, intracellular ADP/ATP ratios or lactate/pyruvate ratios.

Despite having evidence of possible O_2 debt as a precursor for hyperlactatemia, our sampling protocol did not allow us to identify their temporal relationships more precisely. The analysis of BE provided further insight into this matter. We used BE to evaluate other possible ion shifts during the shock period that would not be detected by measuring and analyzing lactate. We observed that CC animals had BE changes consistent with an increased acid load, whereas NoCC animals never had BE lower than 0 (neutral). Furthermore, changes in BE in CC animals occurred as early as B30, which suggests that the increment seen in LIR at B90-R0 is at least in part secondary to energetic failure leading to cellular acidosis and not entirely to a washout phenomenon. This data also provides proof of temporal relationship between these events, placing metabolic acidosis/hyperlactatemia preceding actual vasodilatation.

Finally, the presence of adrenal insufficiency can also explain the lack of responsiveness of the vascular smooth muscle to the presence of vasoconstrictor ligands (13, 39). Adrenal insufficiency can cause vasodilatation mainly by a decreased cortisol stress response. Cortisol stimulates vascular responsiveness by potentiating the vasoconstrictor actions (12, 26, 32, 48) of norepinephrine (by a non-receptor mediated, unclear mechanism) and angiotensin II (by up regulation of angiotensin II receptors in the vascular smooth muscle membrane) (45, 46). A deficient cortisol response results in vascular hyporesponsiveness to pressors and also in more indirect findings such as hypoglycemia. We did not measure adrenal function in our experiment. However, indirect findings provide information to propose testable hypotheses. Our data showed that vasodilatation occurred in the group of animals with highest levels of Epi (CC group), which could be indirect evidence of vascular hyporesponsiveness to adrenal insufficiency, but does not provide proof of principle or causality. In addition, there were no differences in glucose levels between CC and NoCC. On the other hand, the subgroup analysis by survival showed that NS had consistently lower levels of Epi and glucose than S even before hemorrhage (data not shown), suggesting a potential endocrine failure manifested during the surgical procedure before shock.

Limitations

Besides the limitations described above, our major practical limitation was the small number of NoCC animals. Only 3 animals had NoCC and 5 animals did not survive our resuscitation protocol. This small number of NoCC and NS animals represents a limitation when drawing conclusions on the comparison between CC and NoCC, as well as between S and NS.

In conclusion, we describe here a severe T/HS model that mimics the real life trauma conditions and precipitates CC in a majority of the test animals. Furthermore we observed that CC was always preceded by a decrease in VTI and a higher EPI than Non-CC animals and that the LIR rise markedly increased prior to CC. These data collectively support the hypothesis that loss of vasomotor tone precedes CC and that the mechanisms for CC is cellular energy failure owing to an increasing O₂ debt which displays a different threshold value among subjects.

Acknowledgments

This grant was supported in part by NIH grants HL76157 and HL67181. Doctors Yoram Vodovotz, Linda Hermus, Rajaie Namas and Andres Torres were supported by NIH grants GM53789 and HL089082, and Dr. Sven Zenker by Deutsche Forschungsgemeinschaft under grant ZE 904/2-1.

The authors would like to thank Lisa Gordon, MS and Don Severyn, MS for their excellent technical assistance in performing these studies and in data collection.

References

1. Aboab J, Polito A, Orlikowski D, Sharshar T, Castel M, Annane D. Hydrocortisone effects on cardiovascular variability in septic shock: a spectral analysis approach. *Crit Care Med*. 2008; 36:1481–1486. [PubMed: 18434902]
2. Annane D. Corticosteroids for sepsis: controversial forever? *J Crit Care*. 2007; 22:329–330. [PubMed: 18086405]
3. Annane D. Glucocorticoids in the treatment of severe sepsis and septic shock. *Curr Opin Crit Care*. 2005; 11:449–453. [PubMed: 16175031]
4. Annane D, Bellissant E, Bollaert PE, Briegel J, Keh D, Kupfer Y. Corticosteroids for severe sepsis and septic shock: a systematic review and meta-analysis. *Bmj*. 2004; 329:480. [PubMed: 15289273]
5. Annane D, Briegel J, Sprung CL. Corticosteroid insufficiency in acutely ill patients. *N Engl J Med*. 2003; 348:2157–2159. [PubMed: 12761380]
6. Annane D, Fan E, Herridge MS. Pro-con debate: steroid use in ACTH non-responsive septic shock patients with high baseline cortisol levels. *Crit Care*. 2006; 10:210. [PubMed: 16620371]
7. Annane D, Maxime V, Ibrahim F, Alvarez JC, Abe E, Boudou P. Diagnosis of adrenal insufficiency in severe sepsis and septic shock. *Am J Respir Crit Care Med*. 2006; 174:1319–1326. [PubMed: 16973979]
8. Annane D, Seville V, Bellissant E. Effect of low doses of corticosteroids in septic shock patients with or without early acute respiratory distress syndrome. *Crit Care Med*. 2006; 34:22–30. [PubMed: 16374152]
9. Annane D, Seville V, Charpentier C, Bollaert PE, Francois B, Korach JM, Capellier G, Cohen Y, Azoulay E, Troche G, Chaumet-Riffaut P, Bellissant E. Effect of treatment with low doses of hydrocortisone and fludrocortisone on mortality in patients with septic shock. *Jama*. 2002; 288:862–871. [PubMed: 12186604]
10. Astiz ME, Rackow EC, Kaufman B, Falk JL, Weil MH. Relationship of oxygen delivery and mixed venous oxygenation to lactic acidosis in patients with sepsis and acute myocardial infarction. *Crit Care Med*. 1988; 16:655–658. [PubMed: 3371040]
11. Barbee RW, Reynolds PS, Ward KR. Assessing shock resuscitation strategies by oxygen debt repayment. *Shock*. 33:113–122. [PubMed: 20081495]

12. Berecek KH, Bohr DF. Whole body vascular reactivity during the development of deoxycorticosterone acetate hypertension in the pig. *Circ Res.* 1978; 42:764–771. [PubMed: 657435]
13. Carey LC, Curtin R, Sapira JD. Influence of hemorrhage on adrenal secretion, blood glucose and serum insulin in the awake pig. *Ann Surg.* 1976; 183:185–192. [PubMed: 1247317]
14. Chang CG, Van Way CW 3rd, Dhar A, Helling T Jr, Hahn Y. The use of insulin and glucose during resuscitation from hemorrhagic shock increases hepatic ATP. *J Surg Res.* 2000; 92:171–176. [PubMed: 10896818]
15. Cohn SM, Nathens AB, Moore FA, Rhee P, Puyana JC, Moore EE, Beilman GJ. Tissue oxygen saturation predicts the development of organ dysfunction during traumatic shock resuscitation. *The Journal of trauma.* 2007; 62:44–54. discussion 54–45. [PubMed: 17215732]
16. Crookes BA, Cohn SM, Bloch S, Amortegui J, Manning R, Li P, Proctor MS, Hallal A, Blackburne LH, Benjamin R, Soffer D, Habib F, Schulman CI, Duncan R, Proctor KG. Can near-infrared spectroscopy identify the severity of shock in trauma patients? *The Journal of trauma.* 2005; 58:806–813. discussion 813–806. [PubMed: 15824660]
17. Crookes BA, Cohn SM, Burton EA, Nelson J, Proctor KG. Noninvasive muscle oxygenation to guide fluid resuscitation after traumatic shock. *Surgery.* 2004; 135:662–670. [PubMed: 15179373]
18. Davies NW. Modulation of ATP-sensitive K⁺ channels in skeletal muscle by intracellular protons. *Nature.* 1990; 343:375–377. [PubMed: 2153936]
19. De Backer D. Lactic acidosis. *Minerva anesthesiologica.* 2003; 69:281–284. [PubMed: 12766720]
20. Evans DA, Jacobs DO, Wilmore DW. Tumor necrosis factor enhances glucose uptake by peripheral tissues. *Am J Physiol.* 1989; 257:R1182–1189. [PubMed: 2589544]
21. Gannon TA, Britt RC, Weireter LJ, Cole FJ, Collins JN, Britt LD. Adrenal insufficiency in the critically ill trauma population. *Am Surg.* 2006; 72:373–376. [PubMed: 16719187]
22. Gomez, H.; Hermus, L.; Zenker, S.; Polanco, P.; Namas, R.; Vodovotz, Y.; Clermont, G.; Pinsky, MR.; Puyana, JC. American Association for the Surgery of Trauma (AAST). 2008. Sympathetic failure and loss of compensatory response after severe hemorrhage.
23. Helling TS. The liver and hemorrhagic shock. *J Am Coll Surg.* 2005; 201:774–783. [PubMed: 16256922]
24. Kelley KW, Curtis SE, Marzan GT, Karara HM, Anderson CR. Body surface area of female swine. *J Anim Sci.* 1973; 36:927–930. [PubMed: 4703721]
25. Keung EC, Li Q. Lactate activates ATP-sensitive potassium channels in guinea pig ventricular myocytes. *J Clin Invest.* 1991; 88:1772–1777. [PubMed: 1939661]
26. Kurland GS, Freedberg AS. The potentiating effect of ACTH and of cortisone of pressor response to intravenous infusion of L-nor-epinephrine. *Proc Soc Exp Biol Med.* 1951; 78:28–31. [PubMed: 14891908]
27. Landry DW, Oliver JA. The pathogenesis of vasodilatory shock. *N Engl J Med.* 2001; 345:588–595. [PubMed: 11529214]
28. Laubach VE, Shesely EG, Smithies O, Sherman PA. Mice lacking inducible nitric oxide synthase are not resistant to lipopolysaccharide-induced death. *Proc Natl Acad Sci U S A.* 1995; 92:10688–10692. [PubMed: 7479866]
29. Leverve XM. Mitochondrial function and substrate availability. *Crit Care Med.* 2007; 35:S454–460. [PubMed: 17713393]
30. MacMicking JD, Nathan C, Hom G, Chartrain N, Fletcher DS, Trumbauer M, Stevens K, Xie QW, Sokol K, Hutchinson N, et al. Altered responses to bacterial infection and endotoxic shock in mice lacking inducible nitric oxide synthase. *Cell.* 1995; 81:641–650. [PubMed: 7538909]
31. Morales D, Madigan J, Cullinane S, Chen J, Heath M, Oz M, Oliver JA, Landry DW. Reversal by vasopressin of intractable hypotension in the late phase of hemorrhagic shock. *Circulation.* 1999; 100:226–229. [PubMed: 10411844]
32. Pirpiris M, Sudhir K, Yeung S, Jennings G, Whitworth JA. Pressor responsiveness in corticosteroid-induced hypertension in humans. *Hypertension.* 1992; 19:567–574. [PubMed: 1592452]

33. Porter MH, Cutchins A, Fine JB, Bai Y, DiGirolamo M. Effects of TNF-alpha on glucose metabolism and lipolysis in adipose tissue and isolated fat-cell preparations. *J Lab Clin Med.* 2002; 139:140–146. [PubMed: 11944024]
34. Quayle JM, Nelson MT, Standen NB. ATP-sensitive and inwardly rectifying potassium channels in smooth muscle. *Physiol Rev.* 1997; 77:1165–1232. [PubMed: 9354814]
35. Rixen D, Siegel JH. Bench-to-bedside review: oxygen debt and its metabolic correlates as quantifiers of the severity of hemorrhagic and post-traumatic shock. *Crit Care.* 2005; 9:441–453. [PubMed: 16277731]
36. Robin JK, Oliver JA, Landry DW. Vasopressin deficiency in the syndrome of irreversible shock. *J Trauma.* 2003; 54:S149–154. [PubMed: 12768118]
37. Romand JA, Attewell JV, Pinsky MR. Increases in peripheral oxygen demand affect blood flow distribution in hemorrhaged dogs. *Am J Respir Crit Care Med.* 1996; 153:203–210. [PubMed: 8542117]
38. Ronco JJ, Fenwick JC, Tweeddale MG, Wiggs BR, Phang PT, Cooper DJ, Cunningham KF, Russell JA, Walley KR. Identification of the critical oxygen delivery for anaerobic metabolism in critically ill septic and nonseptic humans. *JAMA.* 1993; 270:1724–1730. [PubMed: 8411504]
39. Rushing GD, Britt RC, Britt LD. Effects of hemorrhagic shock on adrenal response in a rat model. *Ann Surg.* 2006; 243:652–654. discussion 654–656. [PubMed: 16633000]
40. Rushing GD, Britt RC, Collins JN, Cole FJ, Weireter LJ, Britt LD. Adrenal insufficiency in hemorrhagic shock. *Am Surg.* 2006; 72:552–554. [PubMed: 16808213]
41. Schlichtig R, Kramer DJ, Pinsky MR. Flow redistribution during progressive hemorrhage is a determinant of critical O₂ delivery. *J Appl Physiol.* 1991; 70:169–178. [PubMed: 2010373]
42. Singer M. Mitochondrial function in sepsis: acute phase versus multiple organ failure. *Crit Care Med.* 2007; 35:S441–448. [PubMed: 17713391]
43. Sprung CL, Annane D, Keh D, Moreno R, Singer M, Freivogel K, Weiss YG, Benbenishty J, Kalenka A, Forst H, Laterre PF, Reinhart K, Cuthbertson BH, Payen D, Briegel J. Hydrocortisone therapy for patients with septic shock. *N Engl J Med.* 2008; 358:111–124. [PubMed: 18184957]
44. Torres LN, Torres Filho IP, Barbee RW, Tiba MH, Ward KR, Pittman RN. Systemic responses to prolonged hemorrhagic hypotension. *Am J Physiol Heart Circ Physiol.* 2004; 286:H1811–1820. [PubMed: 14726303]
45. Ullian ME, Fine JJ. Mechanisms of enhanced angiotensin II-stimulated signal transduction in vascular smooth muscle by aldosterone. *J Cell Physiol.* 1994; 161:201–208. [PubMed: 7962104]
46. Ullian ME, Schelling JR, Linas SL. Aldosterone enhances angiotensin II receptor binding and inositol phosphate responses. *Hypertension.* 1992; 20:67–73. [PubMed: 1618554]
47. Wei XQ, Charles IG, Smith A, Ure J, Feng GJ, Huang FP, Xu D, Muller W, Moncada S, Liew FY. Altered immune responses in mice lacking inducible nitric oxide synthase. *Nature.* 1995; 375:408–411. [PubMed: 7539113]
48. Whitworth JA, Connell JM, Lever AF, Fraser R. Pressor responsiveness in steroid-induced hypertension in man. *Clin Exp Pharmacol Physiol.* 1986; 13:353–358. [PubMed: 3015460]
49. Zenker S, Polanco PM, Kim HK, Torres A, Vodovotz Y, Clermont G, Pinsky MR, Severyn DA, Puyana JC. Thresholded area over the curve of spectrometric tissue oxygen saturation as an indicator of volume resuscitability in porcine hemorrhagic shock. *J Trauma.* 2007; 63:573–578. discussion 578–580. [PubMed: 18073603]

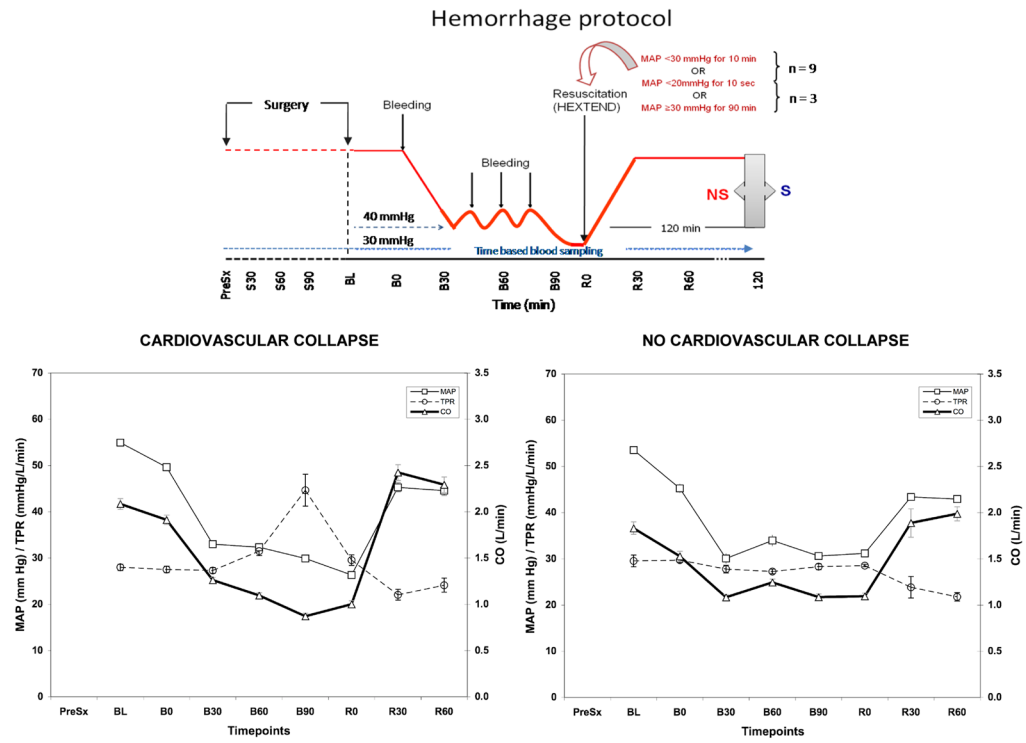
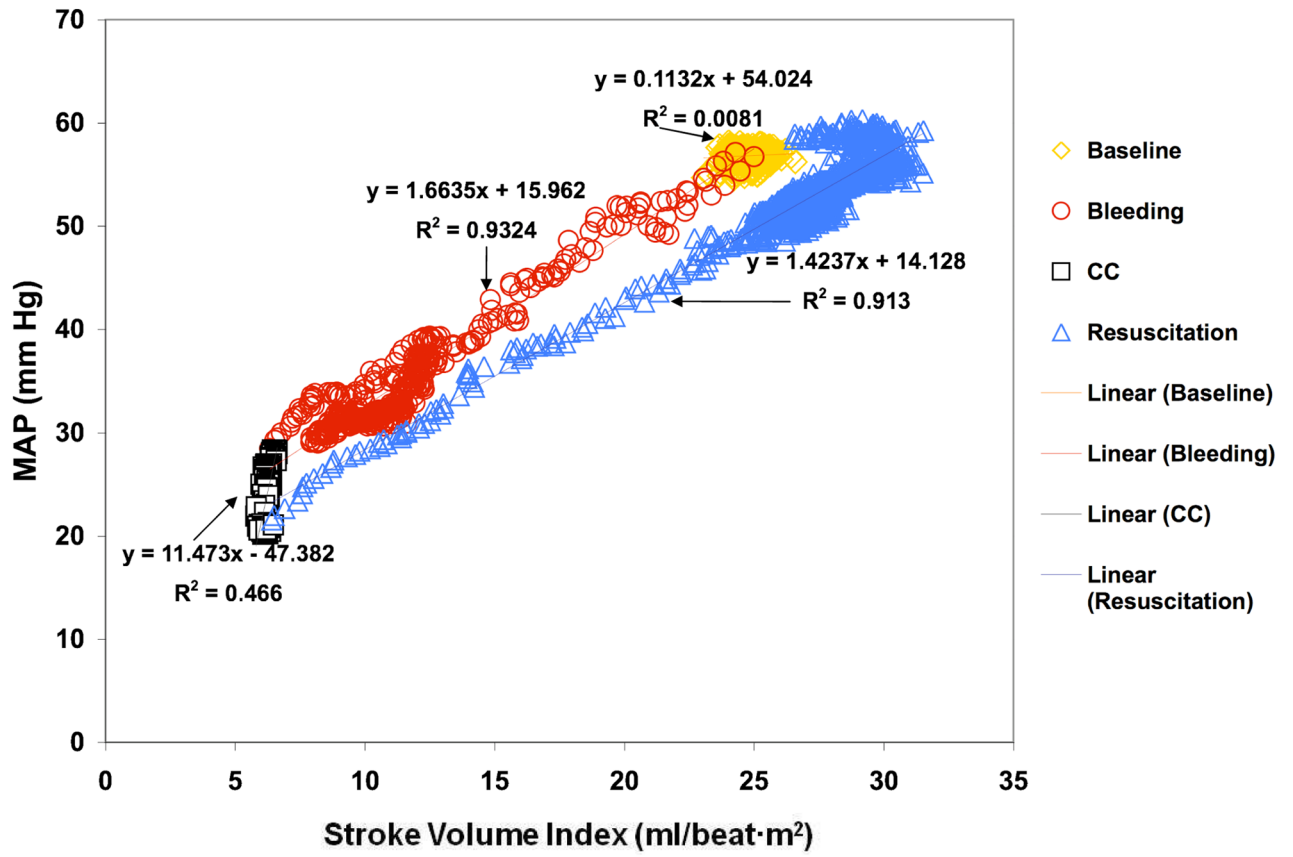


Figure 1. Schematic representation of the hemorrhagic shock protocol (above). Mean arterial pressure (MAP), Total peripheral resistance (TPR) and Cardiac Output (CO) trends during the experiment for CC and NoCC animals.

CARDIOVASCULAR COLLAPSE



CARDIOVASCULAR COLLAPSE

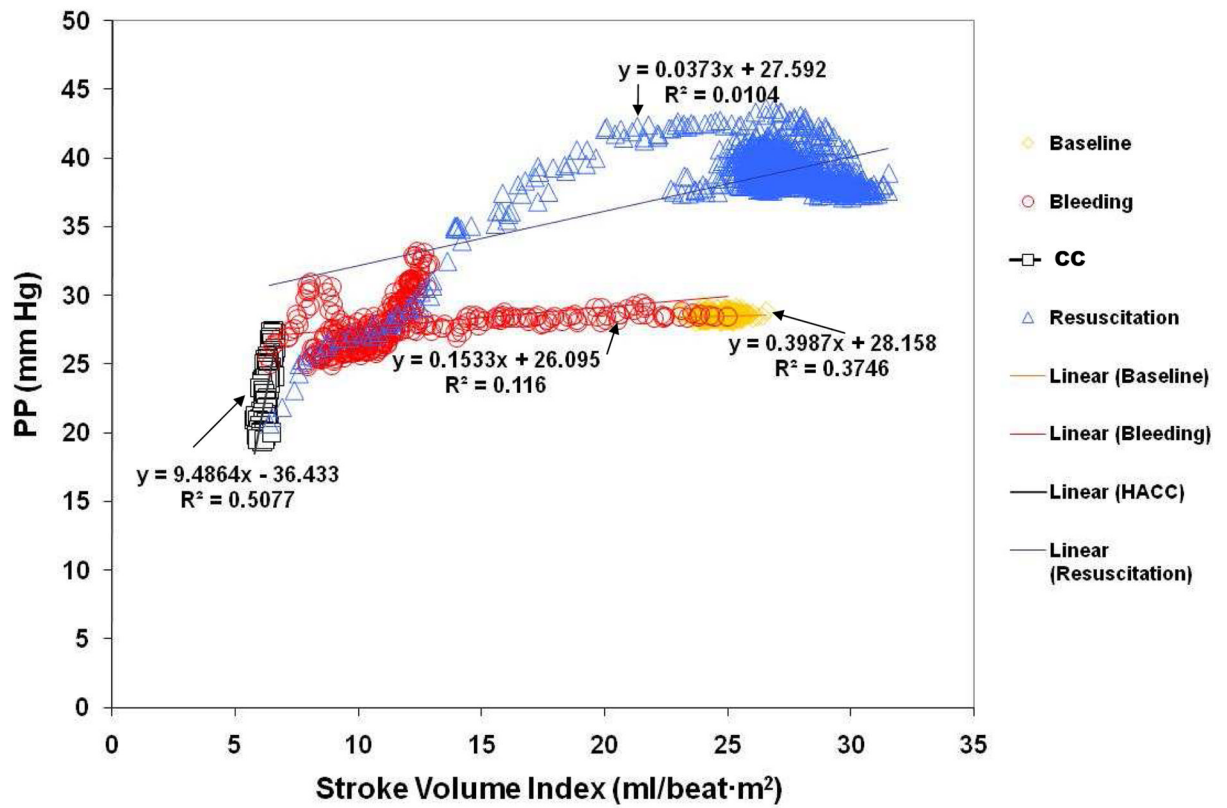
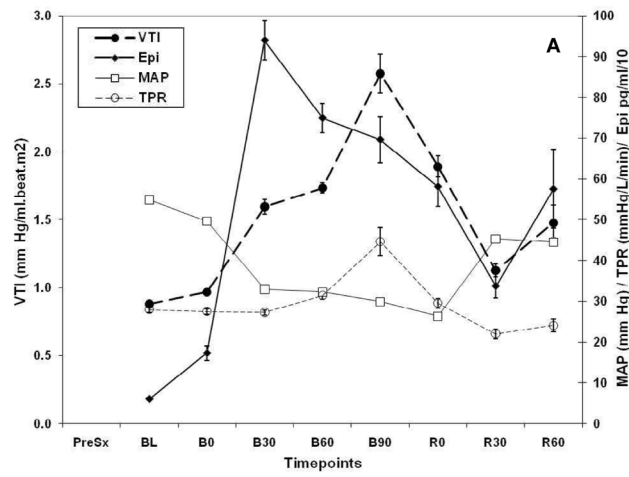
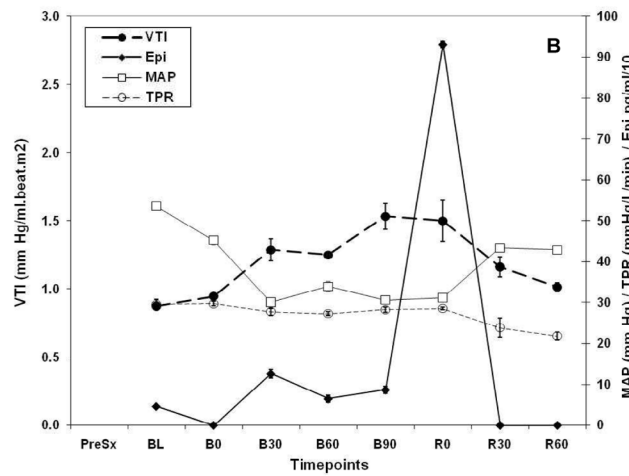


Figure 2.

Figure 2A. Graph representing the pressure/flow relationships using MAP/Stroke volume index (Figure 2A), and using Pulse Pressure/Stroke volume index (Figure 2B) in a CC animal during the stabilization period (yellow diamonds), hemorrhage (red circles), CC (black squares) and resuscitation (blue triangles).



CARDIOVASCULAR COLLAPSE



NO CARDIOVASCULAR COLLAPSE

Figure 3. Graph representing the relationships between VTI, Epi, MAP and TPR throughout the experiment in CC and NoCC animals.

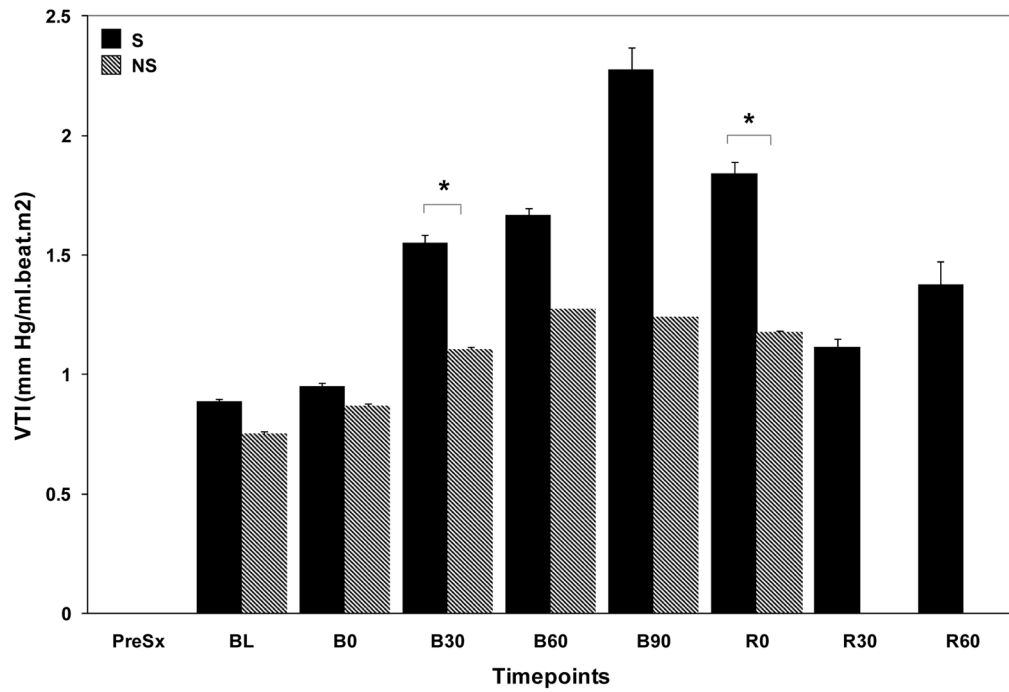


Figure 4. Bar chart showing vasomotor tone measured by VTI in S and NS.

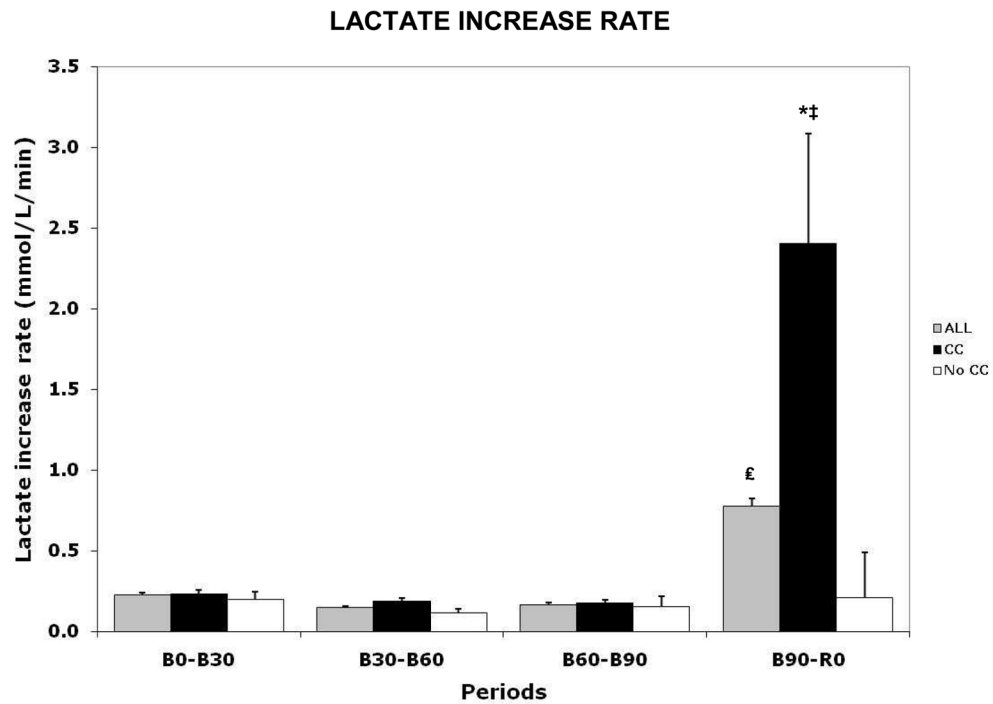
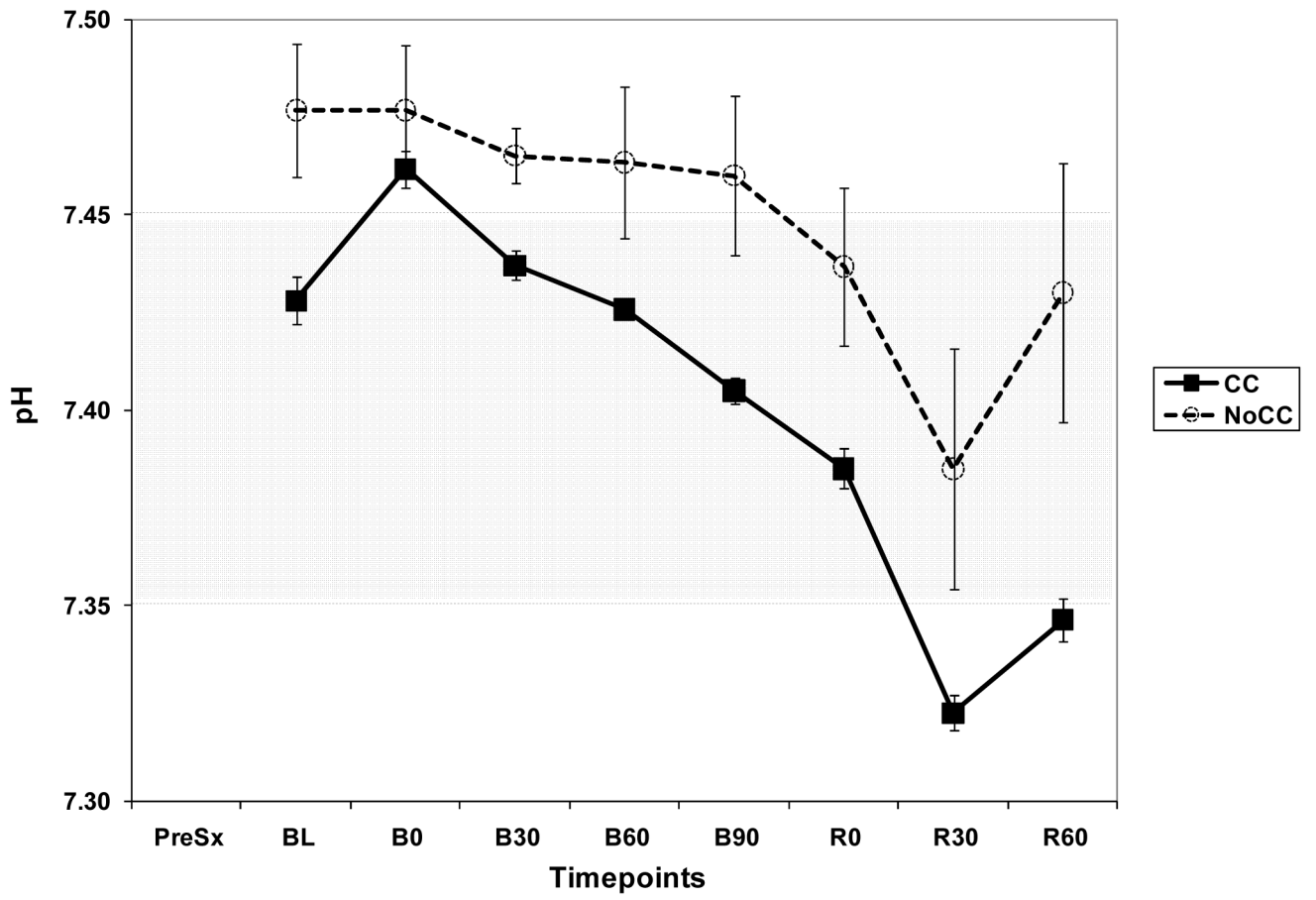


Figure 5. Graph representing lactate increase rate in the entire cohort (ALL), as well as in CC and NoCC groups. * = p value between CC and NoCC, $p < 0.034$; ‡ = p value of LIR between all time points in the CC group, $p = 0.051$; £ = p value between time points B60-B90 and B90-R0, $p = 0.046$.



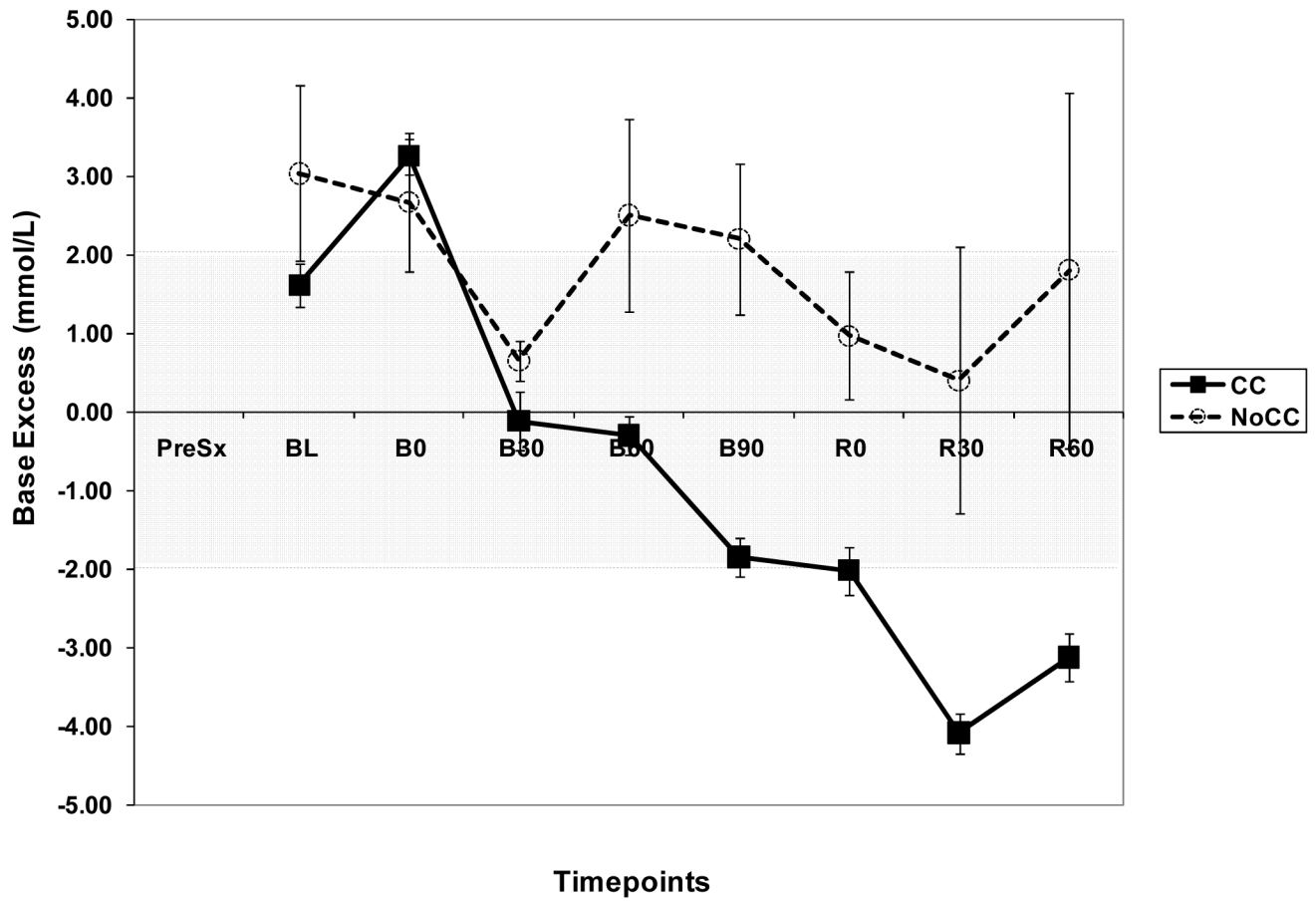


Figure 6.

Figure 6A. Graph showing pH trend during the experiment in CC and NoCC animals.

Figure 6B. Graph showing base excess (BE) trend during the experiment in CC and NoCC animals.

Table 1

Hemodynamic characteristics during surgery and bleeding

Characteristic	Cohort	CC	No CC
n	14	11	3
Excluded animals[‡]	2	2	0
Weight (kg)	31.6 ± 3.7	30.6 ± 1.3	35.0 ± 7.8
Total Blood Volume (ml)	2127 ± 252	2063 ± 87	2355 ± 525
Survivors (n, %)	9/14 (64%)	7/11 (64%)	2/3 (67%)
Surgery period (prior to hemorrhage)			
Duration of Surgery	182.2 ± 27.1	181.9 ± 29.2	175.6 ± 18.6
Hemodynamics during surgery			
HR (beats/min)	113 ± 18	110 ± 10	128 ± 39
30 min			
MAP (mmHg)	64 ± 14	66 ± 16	59 ± 7
SpO₂ (%)	98 ± 1	98 ± 1	97 ± 1
HR (beats/min)	102 ± 12	104 ± 12	95 ± 13
MAP (mmHg)	69 ± 8	69 ± 9	69 ± 8
SpO₂ (%)	96 ± 6	96 ± 7	97 ± 3
90 min			
CI (L/min/m²)	6.2 ± 1.6	6.4 ± 1.7	5.4 ± 0.1
IDO₂ (mlO₂/min/m²)	790 ± 186	814 ± 195	707 ± 178
SvO₂ (%)	70 ± 8	67 ± 7	77 ± 8
Lactate (mmol/L)	1.3 ± 0.3	1.3 ± 0.4	1.4 ± 0.5
HR (beats/min)	94 ± 13	96 ± 15	89 ± 5
MAP (mmHg)	59 ± 5	59 ± 5	59 ± 10
SpO₂ (%)	99 ± 1	99 ± 1	98 ± 1
150 min			
CI (L/min/m²)	4.1 ± 0.7	4.3 ± 0.6	3.4 ± 0.5
IDO₂ (mlO₂/min/m²)	551 ± 86	577 ± 64	476 ± 125
SvO₂ (%)	62 ± 9	62 ± 7	63 ± 18
Shock period			
No. Bleedings	2.1 ± 0.8	2.2 ± 0.9	1.7 ± 0.6
Volume bled (mL)	684 ± 167	722 ± 154	544 ± 159
Volume bled/bleeding (mL)	370 ± 142	379 ± 158	337 ± 65
% Total Blood Volume Bled	32 ± 9	35 ± 8	23 ± 4 *
Time to Decompensation (min)	52.8 ± 31.5	42.3 ± 26.8	91.6 ± 1.6 *
Total duration of Shock (min)	90.8 ± 33.7	80.8 ± 28.1	127.4 ± 29.8 *

Data presented as mean ± SD;

* p > 0.05 as compared to CC.

[‡]Two animals were excluded from the study, the first due to an error in the hemodynamic data collection system. The second was excluded because of profound metabolic derangement after surgery but before hemorrhage, presumably due to malignant hyperthermia.

Table 2

Hemodynamic and cardiac parameters after surgery and during hemorrhage

	Hemodynamic and cardiac parameters									
	BL	B0	B30	B60	B90	R0	R30	R60		
PP (mmHg)										
All	25.7 ± 3.1	24.7 ± 4.4	22.4 ± 4.4	22.4 ± 3.0	22.0 ± 2.5	22.0 ± 2.8	30.3 ± 7.9	30.2 ± 7.4		
CC	26 ± 3.5	25.7 ± 4.5	23.3 ± 4.4	22.9 ± 3.1	22.4 ± 1.0	22.2 ± 3.0	30.9 ± 8.8	30.9 ± 8.2		
No CC	24.5 ± 1.1	21.6 ± 2.9	19.5 ± 3.6	20.9 ± 2.9	21.5 ± 4.1	21.6 ± 2.1	28.1 ± 1.5	27.4 ± 2.7		
SVI (ml/m²)										
All	30.4 ± 6.0	26.5 ± 6.2	15.8 ± 3.6	14.2 ± 3.2	11.9 ± 4.0	13.1 ± 5.9	29.1 ± 11.1	28.6 ± 10.2		
CC	31.2 ± 7.0	27.8 ± 6.9	16.0 ± 4.2	13.2 ± 3.4	10.1 ± 3.5	12.3 ± 6.6	30.3 ± 11.9	29.0 ± 12.2		
No CC	28.2 ± 1.7	22.9 ± 3.3	15.3 ± 1.9	16.7 ± 1.7	14.4 ± 3.8	15.4 ± 4.9	24.7 ± 3.4	27.1 ± 0.3		
HR (bpm)										
All	98 ± 18	101 ± 15	113 ± 19	116 ± 18	114 ± 17	114 ± 17	110 ± 16	113 ± 19		
CC	101 ± 19	105 ± 15	119 ± 18	123 ± 16	122 ± 18	118 ± 17	113 ± 16	118 ± 18		
No CC	87 ± 8	89 ± 9	95 ± 3 *	99 ± 11	103 ± 8	101 ± 14	97 ± 7	94 ± 5		
IDO₂ (mlO₂/min/m²)										
All	412 ± 129	350 ± 107	236 ± 36	215 ± 40	185 ± 61	165 ± 55	248 ± 92	226 ± 81		
CC	439 ± 134	387 ± 105	241 ± 38	211 ± 38	176 ± 72	161 ± 57	254 ± 97	228 ± 86		
No CC	320 ± 51	266 ± 57	209 ± 48	228 ± 49	197 ± 55	179 ± 56	227 ± 83	216 ± 84		
IVO₂ (mlO₂/min/m²)										
All	161 ± 56	171 ± 56	143 ± 54	143 ± 45	136 ± 43	111 ± 55	95 ± 77	100 ± 80		
CC	178 ± 56	191 ± 58	144 ± 60	141 ± 51	136 ± 56	105 ± 60	97 ± 81	104 ± 84		
No CC	112 ± 16	132 ± 24	141 ± 20	146 ± 38	137 ± 30	131 ± 28	87 ± 78	87 ± 78		
O₂ER (%)										
All	0.42 ± 0.10	0.51 ± 0.06	0.68 ± 0.08	0.65 ± 0.16	0.74 ± 0.05	0.75 ± 0.14	0.57 ± 0.20	0.68 ± 0.19		
CC	0.44 ± 0.10	0.51 ± 0.06	0.68 ± 0.08	0.66 ± 0.19	0.77 ± 0.02	0.75 ± 0.16	0.56 ± 0.23	0.70 ± 0.21		
No CC	0.36 ± 0.10	0.50 ± 0.09	0.67 ± 0.08	0.64 ± 0.04	0.71 ± 0.06	0.74 ± 0.07	0.60 ± 0.10	0.62 ± 0.10		
SvO₂ (%)										
All	52 ± 8	48 ± 8	27 ± 9	31 ± 16	22 ± 6	24 ± 13	35 ± 10	35 ± 11		

Hemodynamic and cardiac parameters									
	BL	B0	B30	B60	B90	R0	R30	R60	
CC	51 ± 9	49 ± 8	26 ± 9	31 ± 20	19 ± 2	23 ± 14	35 ± 12	35 ± 12	
No CC	53 ± 6	47 ± 9	31 ± 6	33 ± 4	26 ± 6	25 ± 7	36 ± 8	36 ± 11	
StO₂ (%)									
All	79 ± 6	80 ± 6	78 ± 6	77 ± 7	77 ± 7	77 ± 7	76 ± 21	85 ± 5	
CC	80 ± 7	81 ± 7	79 ± 7	78 ± 9	79 ± 9	78 ± 8	83 ± 9	85 ± 5	
No CC	77 ± 5	76 ± 5	74 ± 3	75 ± 3	75 ± 3	76 ± 4	60 ± 36	82 ± 5	
VTI (mmHg/mL-beat·m²)									
All	0.9 ± 0.2	0.9 ± 0.2	1.4 ± 0.4	1.6 ± 0.4	2.1 ± 1.2	1.7 ± 0.6	1.1 ± 0.4	1.4 ± 1.2	
CC	0.9 ± 0.2	0.9 ± 0.2	1.5 ± 0.5	1.7 ± 0.4*	2.6 ± 1.4	1.9 ± 0.8	1.1 ± 0.5	1.5 ± 1.4	
No CC	0.9 ± 0.1	0.9 ± 0.02	1.3 ± 0.2	1.3 ± 0.1	1.5 ± 0.3	1.5 ± 0.5	1.2 ± 0.2	1.0 ± 0.1	

Data presented as Mean ± SD;

* p < 0.05 comparing CC to No CC.

Table 3

Sympathetic, endocrine, immunologic and metabolic variables

	Sympathetic/endocrine, immunologic and metabolic parameters										
	BL	B0	B30	B60	B90	R0	R30	R60			
Epinephrine (ng/ml)											
All	55.9 ± 307.8	129.9 ± 172.8	668.4 ± 564.2	521.1 ± 767.9	492.9 ± 451.6	712.1 ± 624.6	270.0 ± 289.1	460.2 ± 873.8			
CC	60.7 ± 36.2	173.2 ± 181.0	939.7 ± 474.7	749.3 ± 365.8	696.0 ± 564.7	581.2 ± 482.9	337.5 ± 284.6	575.2 ± 964.2			
No CC	46.3 ± 80.2	ND [§]	126 ± 218.2 *	64.7 ± 14.3 *	86.7 ± 122.7 [§]	930.3 ± 885.9	ND	ND			
TNF (pg/ml)											
All	162.6 ± 103.4	162.6 ± 109.3	202.8 ± 137.2	207.3 ± 131.8	194.8 ± 121.6	195.0 ± 118.5	151.0 ± 77.6	155.8 ± 84.2			
CC	171.2 ± 117.6	143.3 ± 120.6	195.0 ± 117.7	203.2 ± 113.9	187.0 ± 98.9	193.0 ± 103.3	140.6 ± 81.8	146.2 ± 88.5			
No CC	145.3 ± 112.2	171.1 ± 166.9	218.7 ± 200.3	215.7 ± 191.9	210.3 ± 184.7	199.0 ± 171.6	177.1 ± 86.1	179.8 ± 69.2			
Base excess (mmol/L)											
All	2.3 ± 2.8	3.1 ± 2.2	0.5 ± 3.2	0.5 ± 2.9	-0.1 ± 3.2	-1.1 ± 3.4	-2.9 ± 3.4	-1.9 ± 4.2			
CC	1.9 ± 2.5	3.2 ± 2.2	0.4 ± 3.5	-0.3 ± 2.4	-1.8 ± 2.5	-1.9 ± 3.2	-3.7 ± 2.5	-2.9 ± 3.2			
No CC	3.0 ± 3.3	2.7 ± 2.7	0.6 ± 0.8	2.5 ± 3.7	2.2 ± 2.9	0.9 ± 2.4	0.4 ± 5.1	1.8 ± 6.8			
pH											
All	7.41 ± 0.14	7.47 ± 0.04	7.41 ± 0.14	7.40 ± 0.14	7.43 ± 0.05	7.39 ± 0.06	7.34 ± 0.06	7.32 ± 0.14			
CC	7.39 ± 0.16	7.46 ± 0.05	7.39 ± 0.15	7.37 ± 0.16	7.40 ± 0.03	7.38 ± 0.05	7.33 ± 0.04	7.29 ± 0.14			
No CC	7.48 ± 0.05	7.48 ± 0.05	7.46 ± 0.02	7.46 ± 0.06	7.46 ± 0.06	7.44 ± 0.06	7.38 ± 0.09	7.43 ± 0.09			
Lactate (mmol/L)											
All	1.6 ± 0.4	1.5 ± 0.3	2.4 ± 0.9	2.8 ± 0.9	3.2 ± 1.0	4.3 ± 1.6	5.9 ± 1.3	5.7 ± 2.0			
CC	1.6 ± 0.4	1.4 ± 0.3	2.4 ± 0.9	3.0 ± 0.8	3.6 ± 1.1	4.6 ± 1.6	6.3 ± 1.3	6.0 ± 1.9			
No CC	1.5 ± 0.5	1.7 ± 0.3	2.3 ± 0.5	2.1 ± 0.7 [§]	2.6 ± 0.4	3.2 ± 0.4	4.6 ± 0.8	4.7 ± 1.9			
Glucose (mg/dl)											
All	55 ± 23	50 ± 21	56 ± 24	60 ± 19	62 ± 23	58 ± 23	76 ± 28	85 ± 35			
CC	54 ± 24	45 ± 22	56 ± 27	59 ± 22	68 ± 33	69 ± 39	82 ± 33	90 ± 38			
No CC	59 ± 13	60 ± 16	53 ± 11	61 ± 14	57 ± 9	57 ± 11	61 ± 5	66 ± 1			

Data presented as Mean ± SD; ND: Not detectable.

* : p<0.05.

§ p=0.06/0.07 comparing CC to No CC.

NIH-PA Author Manuscript

NIH-PA Author Manuscript

NIH-PA Author Manuscript